

The Approach to Stability for Delayed Feedback Control of Chaos for 1-dimensional Maps

J. Keith Thomas and Edward H. Hellen*

University of North Carolina Greensboro,

Department of Physics and Astronomy, Greensboro, NC 27402

(Dated: August 1, 2008)

Abstract

We investigate mathematically and experimentally the approach to stability using the Pyragas delayed proportional feedback control method applied to a chaotic finite difference 1-dimensional map. This method does not use unstable fixed points or require computational analysis and is therefore easy to implement experimentally. For measurements we use an analog electronic circuit realization of a finite difference quadratic return map. Comparison with predictions is facilitated by doing the linear stability analysis in terms of successive system values instead of errors from the fixed point. We find that the behavior of the approach to stability can be smooth and steady or appear erratic depending on the feedback gain.

PACS number(s): 05.45.Gg

*Electronic address: ehhellen@uncg.edu

It is well known that proportional feedback methods can control chaos for systems described by 1-dimensional maps [1, 2, 3, 4]. Typically in these methods a system parameter is perturbed by an amount proportional to the difference between the current system value and the unstable fixed point. Pyragas [5] introduced an alternative in which the perturbation is proportional to the difference between the current system value and a previous system value. This delayed feedback control (DFC) method successfully controls chaotic behavior in a variety of experiments (see references in Ref. [6]). However, little attention has been paid to the approach to stability when control is turned on. Here we apply DFC to finite difference return maps and derive the mathematical form of the approach to stability and verify it experimentally using an electronic circuit previously used to produce real-time bifurcation diagrams for the 1-dimensional Hénon map [7]. We find a variety of behaviors for the approach to stability depending on the gain of the feedback. Some are steady and smooth as the system values converge to the fixed value, while other cases appear to converge somewhat erratically. In all cases the predictions show good agreement with measurements. This knowledge should be useful when the performance of the control is being closely monitored and evaluated.

We consider the 1-dimensional finite difference map for system value x with system parameter a

$$x_{n+1} = f(x_n, a_n). \quad (1)$$

Using the DFC method on successive system values, the perturbation of a_n is

$$\Delta a_n = a_n - a_0 = K(x_n - x_{n-1}) \quad (2)$$

where a_0 is the unperturbed parameter value and K is the feedback gain. Feedback is applied only when the magnitude of $(x_n - x_{n-1})$ is within a specified window for control. This method is based on the idea that in a neighborhood of a fixed point of Eq. (1) the difference between successive system values decreases as the distance from the system value to the fixed value decreases. Therefore DFC has the desired property of the perturbation vanishing when the system value attains the unstable fixed value.

Pyragas has pointed out that DFC is well suited to experimental implementation since it works without knowledge of unstable fixed points or orbits, and does not require computational analysis. Thus DFC has advantages for high speed systems [8] and in situations where the unstable fixed point is not known or changes with time. We note that the application

of DFC using successive system values is essentially a derivative control method since the perturbation uses the difference in system values per iteration [9]. The DFC method used here is also referred to as a discrete version of time-delay autosynchronization [8].

The goal here is to predict the behavior of the convergence of system values caused by the control algorithm in Eq. (2). The unperturbed return map is $x_{n+1} = f(x_n, a_0)$. The fixed point x^* satisfies $x^* = f(x^*, a_0)$. Chaotic behavior is stabilized by perturbing parameter a_n about the value a_0 so as to move the system value x towards the unstable fixed point x^* . A linear expansion of $f(x_n, a_n)$ about x^* and a_0 gives

$$x_{n+1} = f(x^*, a_0) + f_x(x_n - x^*) + f_a(a_n - a_0), \quad (3)$$

where f_x and f_a are the partial derivatives. This is rewritten as

$$(x_{n+1} - x^*) = f_x(x_n - x^*) + f_a K(x_n - x_{n-1}), \quad (4)$$

where we included our perturbation Eq. (2). Fixed point x^* is added and subtracted to the third bracketed term and Eq. (4) is rearranged as

$$(x_{n+1} - x^*) = (f_x + f_a K)(x_n - x^*) - f_a K(x_{n-1} - x^*). \quad (5)$$

Instead of solving for the behavior of the error terms $(x_n - x^*)$ we are interested in differences of successive system values $(x_n - x_{n-1})$ since these are directly available from measurements. Therefore we replace n by $n - 1$ in Eq. (5) and then subtract from Eq. (5) to get

$$(x_{n+1} - x_n) = (f_x + f_a K)(x_n - x_{n-1}) - f_a K(x_{n-1} - x_{n-2}). \quad (6)$$

We note that Eqs. (5) and (6) have the same form so that $(x_n - x_{n-1})$ and $(x_n - x^*)$ have the same solution, although their initial conditions will be different. The initial conditions for $(x_n - x_{n-1})$ are readily available from measurements whereas initial conditions for $(x_n - x^*)$ rely on knowledge of x^* .

Let $y_n = x_n - x_{n-1}$ and look for solutions $y_n = s^n$. Equation (6) leads to the characteristic equation

$$s^2 - (f_x + f_a K)s + f_a K = 0. \quad (7)$$

The characteristic multipliers are

$$s_{\pm} = \frac{f_x + f_a K}{2} \pm \sqrt{\left(\frac{f_x + f_a K}{2}\right)^2 - f_a K} \quad (8)$$

giving solution

$$y_n = c_1 s_+^n + c_2 s_-^n. \quad (9)$$

The coefficients c_1 and c_2 are determined by two consecutive measured values (the initial conditions) $y_0 = c_1 + c_2$ and $y_1 = c_1 s_+ + c_2 s_-$. Solving for the coefficients gives

$$c_1 = \frac{-s_- y_0 + y_1}{s_+ - s_-} \quad (10a)$$

$$c_2 = \frac{s_+ y_0 - y_1}{s_+ - s_-}. \quad (10b)$$

With no perturbation ($K = 0$) the characteristic multiplier $s_- = f_x < -1$ in the neighborhood of the fixed point since the unperturbed map gives chaotic behavior. (And $s_+ = 0$.) In order to induce stability a positive $f_a K$ is used in Eq. (8) so that $-1 < s_- < 0$. So for small K (with sign such that $f_a K > 0$) the multipliers in Eq. (8) are negative and real. As the magnitude of K is increased the multipliers merge and become equal when

$$K = \frac{2\sqrt{1 - f_x} - 2 + f_x}{-f_a}. \quad (11)$$

This is the transition between smooth and non-smooth convergence as shown below. For larger values of K the multipliers are the complex conjugates

$$s_{\pm} = \frac{f_x + f_a K}{2} \pm i \sqrt{f_a K - \left(\frac{f_x + f_a K}{2}\right)^2}. \quad (12)$$

Using the Euler representation of the complex roots, $s_{\pm} = r e^{\pm i\phi}$, and taking the form of Eq. (9) the solution is

$$y_n = c (r e^{i\phi})^n + c^* (r e^{-i\phi})^n, \quad (13)$$

where

$$c = \frac{y_0}{2} + i \left(\frac{y_0 \operatorname{Re}(s_+) - y_1}{2 \operatorname{Im}(s_+)} \right) = c_0 e^{i\theta}. \quad (14)$$

Thus the solution is

$$y_n = c_0 e^{i\theta} (r e^{i\phi})^n + c_0 e^{-i\theta} (r e^{-i\phi})^n = 2c_0 r^n \cos(n\phi + \theta), \quad (15)$$

where

$$\phi = \arctan \left(\frac{\sqrt{4f_a K - (f_x + f_a K)^2}}{f_x + f_a K} \right), \quad (16)$$

and

$$\theta = \arctan \left(\frac{y_0 \operatorname{Re}(s_+) - y_1}{y_0 \operatorname{Im}(s_+)} \right). \quad (17)$$

The integer n in the cosine term causes non-smooth convergence distinctly different from the smooth convergence of Eq. (9) that after a few iterations goes as s_-^n (since $s_- < s_+ < 0$).

Equation (9) converges to zero as long as $s_- > -1$. Stability analysis gives the condition

$$f_a K > \frac{-1 - f_x}{2}. \quad (18)$$

Thus the smallest value of K that controls chaos is

$$K_{small} = \frac{1 + f_x}{-2f_a}. \quad (19)$$

Convergence of Eq. (15) occurs when $r < 1$, thus the largest K that controls chaos is

$$K_{large} = 1/f_a. \quad (20)$$

The result is that we predict control of chaos for feedback gain K between $(1 + f_x)/(-2f_a)$ and $1/f_a$, with Eq. (11) giving the transition from smooth convergence [Eq. (9)] to non-smooth convergence [Eq. (15)].

As an example we consider the 1-dimensional Hénon map:

$$f(x, a) = 1 - ax^2 \quad (21)$$

with fixed point

$$x^* = \frac{-1 + \sqrt{1 + 4a_0}}{2a_0} \quad (22)$$

and partial derivatives evaluated at (x^*, a_0)

$$f_x = -2a_0 x^* = 1 - \sqrt{1 + 4a_0} \quad (23)$$

$$f_a = -(x^*)^2. \quad (24)$$

For values of a_0 between 1.4 and 2 Eq. (21) displays a variety of unstable behavior including high period oscillations and chaos [7]. For $a_0 = 1.9$ we find $f_x = -1.93$ and $f_a = -0.259$, so convergence is predicted for values of K between -1.8 and -3.87 with the transition from smooth to non-smooth convergence at -1.96.

Figure 1 shows the circuit used to apply the control algorithm to a function block circuit $f(x, a)$ that performs analog computation of a chaotic return map. Here we use the function

block circuit shown in Fig. 2 that calculates the 1-dimensional Hénon map Eq. (21). We have also used function block circuits that produce the Logistic map and the tent map.

At the upper left in Fig. 1 the unperturbed parameter value a_0 is added to the perturbation Δa_n to create system parameter a_n . This is input, along with system value voltage V_n , to the $f(x, a)$ circuit block which produces the next system value voltage V_{n+1} . The subtraction op amp creates the difference between the successive system value voltages ΔV_{n+1} that is used to create Δa_{n+1} , the perturbation for the next iteration. ΔV_{n+1} is passed to an absolute value/comparator stage and to a gain stage which produces Δa_{n+1} . The output of the comparison stage (LM339) controls the gate of the FET in the gain stage so that if $|\Delta V|$ is larger than the control window then the gate goes to -5 volts turning off the FET and thereby setting feedback gain $K = 0$. A nonzero value for K is determined by the inverting op amp adjacent to the FET. For the values shown, $47k\Omega$ and $13k\Omega$, $K = -3.6$. The sign of K is easily switched by changing the order of inputs V_n and V_{n+1} to the subtraction amplifier. Prior to the FET $|\Delta V|$ is divided by 10, the scaling factor of the AD633 multiplier used in the $f(x, a)$ circuit block, to convert from voltage $|\Delta V|$ to $|\Delta x|$. The sample/holds (LF398) perform the iteration under the control of the 555 timer circuit. With the $68k\Omega$ and $0.001\mu f$ shown in the schematic the iteration period is about $100\mu s$.

Data were collected with a Tektronix TDS 3000 oscilloscope. The control circuit was periodically gated on and off (by holding the FET's gate to -5 volts during the off phase, circuitry not shown) so that it was possible to trigger from the gating signal in order to capture the entire control of chaotic behavior. Figures 3 and 4 show measured voltages for the system values $V_n = 10x_n$ and parameter values a_n for $a_0 = 1.9$, a value that gives chaotic behavior. The effect of the gating and the control window are apparent. Control was gated on at $t = 0$ in both cases, but in Fig. 3 $|\Delta V|$ was not within the control window until about $t = 4.5$ ms. Figure 3 uses feedback gain $K = -1.96$ corresponding to the transition [Eq. (11)] between smooth and nonsmooth convergence, and Fig. 4 uses $K = -3.53$ corresponding to non-smooth convergence.

The DFC algorithm uses feedback proportional to the difference between successive system values, $y_n = x_n - x_{n-1}$. When the system is successfully controlled $y_n \rightarrow 0$. The approach to zero for y_n may be smooth and steady [Eq. (9)] or may appear somewhat erratic [Eq. (15)]. Figures 5, 6, and 7 show data and prediction for y_n (actually $\Delta V_n = 10y_n$) for three values of K showing the variety of convergence. Predictions were made by using

two successive measured system value differences for y_0 and y_1 in Eqs. (10) and (14) to determine the coefficients for Eqs. (9) or (15). The convergence in Fig. 5 is smooth and steady, in Fig. 6 it appears somewhat erratic, and in Fig. 7 a pattern is apparent although the convergence is not steady. In all cases there is good agreement between the prediction and measurement.

We note that for simple proportional feedback using parameter perturbation $\Delta a = K(x_n - x^*)$ applied to the Hénon map with $a = 1.9$, the optimal feedback gain is $-f_x/f_a = -1.93/0.259 = -7.45$ [2]. Half of this value is within our predicted range of -1.8 to -3.87 for K using DFC. This is reasonable since the difference from the system value to the fixed point $(x_n - x^*)$ can be expected to typically be about half of $(x_n - x_{n-1})$, so the simple proportional feedback method needs gain about twice that of the DFC gain in order to get a similar perturbation Δa .

We have shown that a variety of behavior is expected for the approach to stability when applying DFC to a finite difference 1-dimensional chaotic map. This may be valuable in situations in which the convergence is being closely monitored since erratic and non-steady behavior could be mistaken for a faulty control mechanism.

Acknowledgments

This research was supported by an award from the Research Corporation. Corey Clift contributed to early work on this project.

-
- [1] E. Ott, C. Grebogi, and J. A. Yorke, *Phys. Rev. Lett.* **64**, 1196-1199 (1990).
 - [2] R. J. Wiener, K. E. Callan, S. C. Hall, and T. Olsen, *Am. J. Phys.* **74**, 200-206 (2006).
 - [3] D. J. Gauthier, *Am. J. Phys.* **71**, 750-759 (2003).
 - [4] C. Flynn and N. Wilson, *Am. J. Phys.* **66**, 730-735 (1998).
 - [5] K. Pyragas, *Phys. Lett. A* **170**, 421-428 (1992).
 - [6] J. E. S. Socolar and D. J. Gauthier, *Phys. Rev. E* **57**, 6589-6595 (1998).
 - [7] E. H. Hellen, *Am. J. Phys.* **72**, 499-502 (2004).
 - [8] J. E. S. Socolar, D. W. Sukow, and D. J. Gauthier, *Phys. Rev. E* **50**, 3245-3248 (1994).
 - [9] P. Parmananda, M. A. Rhode, G. A. Johnson, R. W. Rollins, H. D. Dewald, and A. J. Markworth, *Phys. Rev. E* **49**, 5007-5011 (1994).

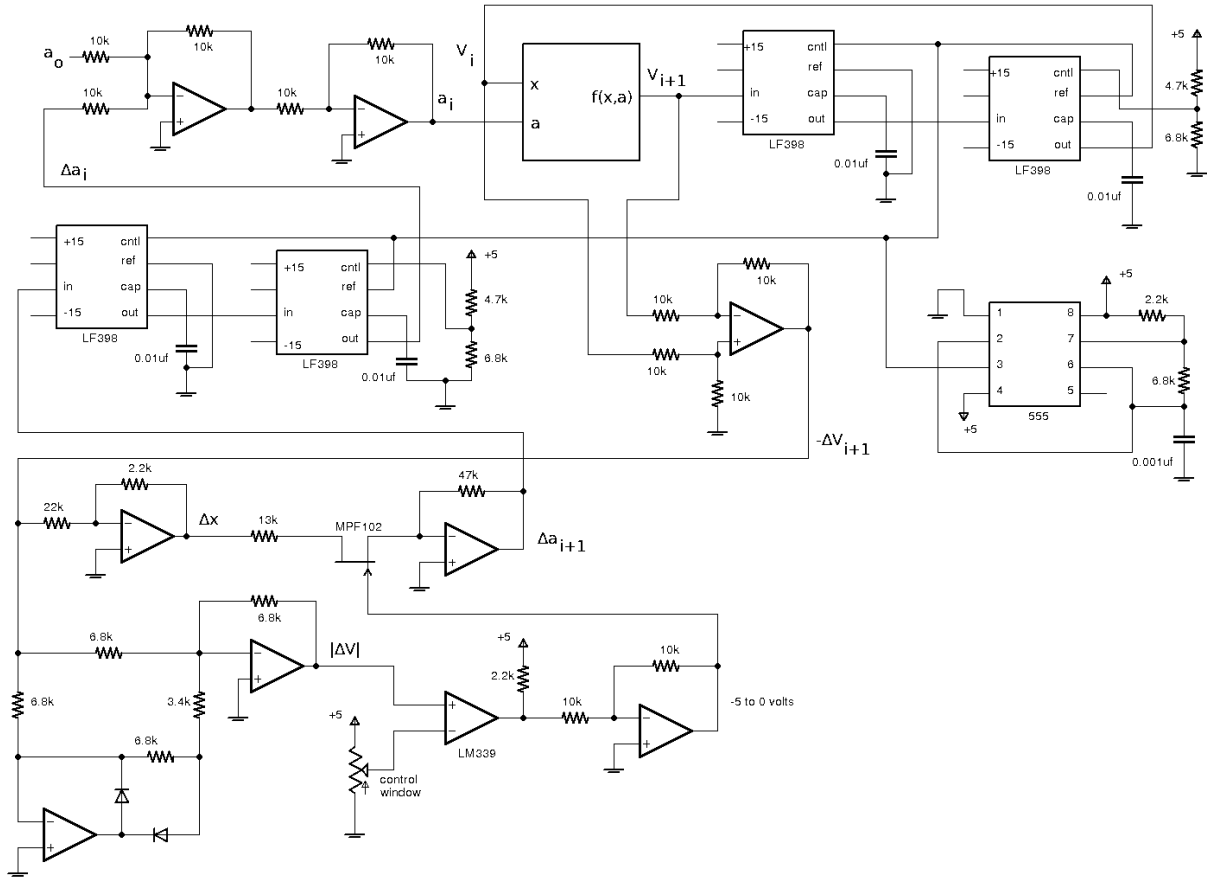


FIG. 1: The circuit for controlling chaotic behavior of the return map $x_{n+1} = f(x_n, a_n)$. Op amps are LF412.

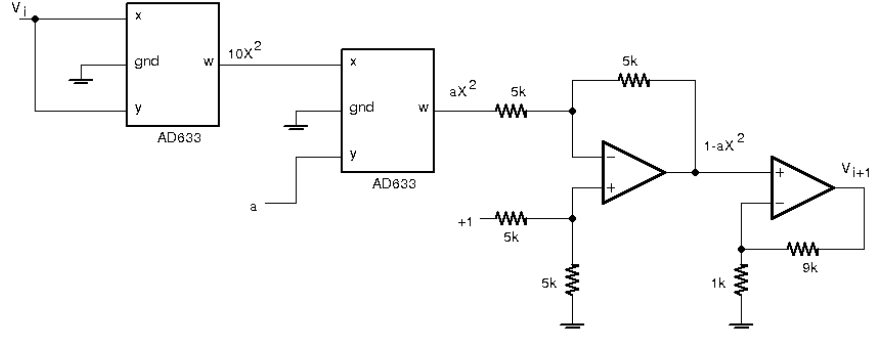


FIG. 2: Henon function block circuit for $f(x, a)$. Relation between voltage and system value is $x = V/10$. The $\times 10$ noninverting amplifier at the output accounts for both a and the $+1$ not being multiplied by 10, the scaling factor of the AD633 multiplier.

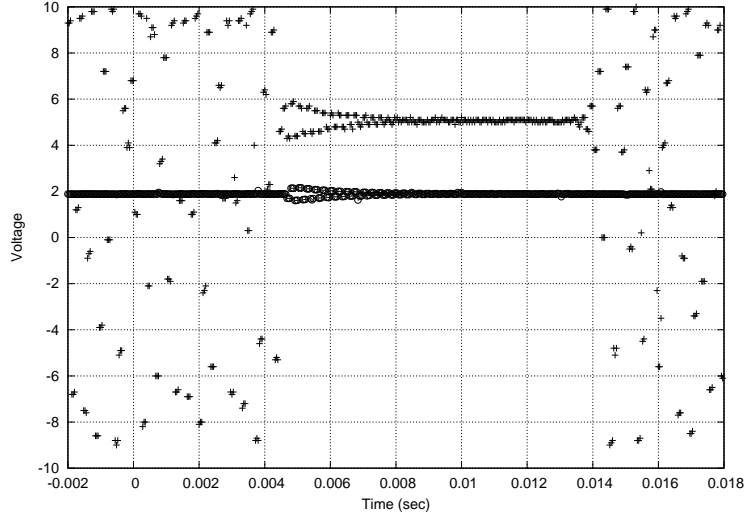


FIG. 3: Measured system value voltages $V_i = 10x_i$ for smooth control of Henon system with feedback gain $K = -1.96$. Control was gated on at $t = 0$ and off at $t = 0.012$. Also shown is the parameter value $a = a_0 + \Delta a$ with $a_0 = 1.9$.

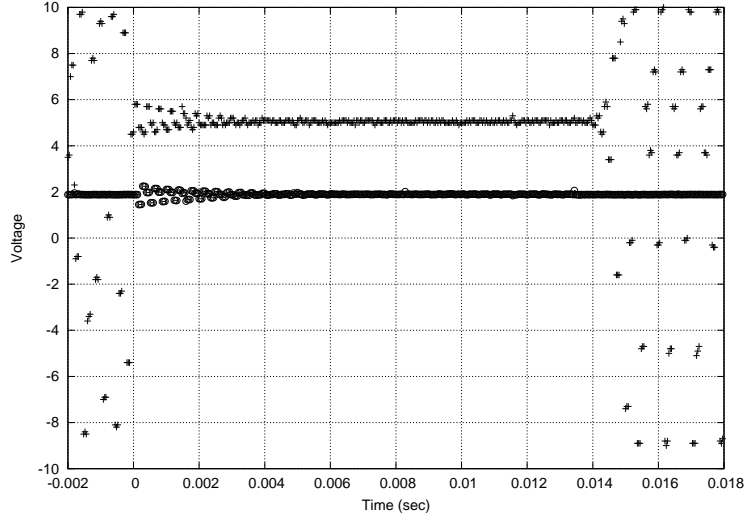


FIG. 4: Measured system value voltages $V_i = 10x_i$ for non-smooth control of Henon system with feedback gain $K = -3.53$. Control was gated on at $t = 0$ and off at $t = 0.012$. Also shown is the parameter value $a = a_0 + \Delta a$ with $a_0 = 1.9$.

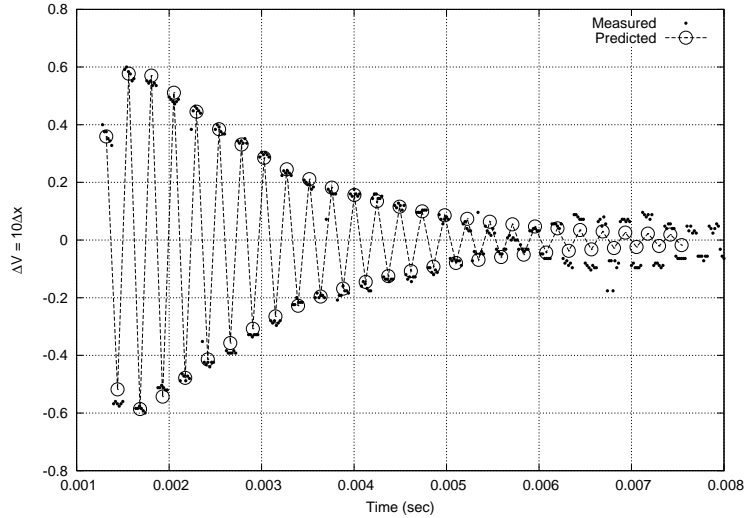


FIG. 5: Data (dots) and prediction (open circles) showing the difference of successive system values $\Delta V_i = 10y_i = 10(x_i - x_{i-1})$ for smooth-convergence, $K = -1.9$. The connecting dashed lines are for visual aid only.

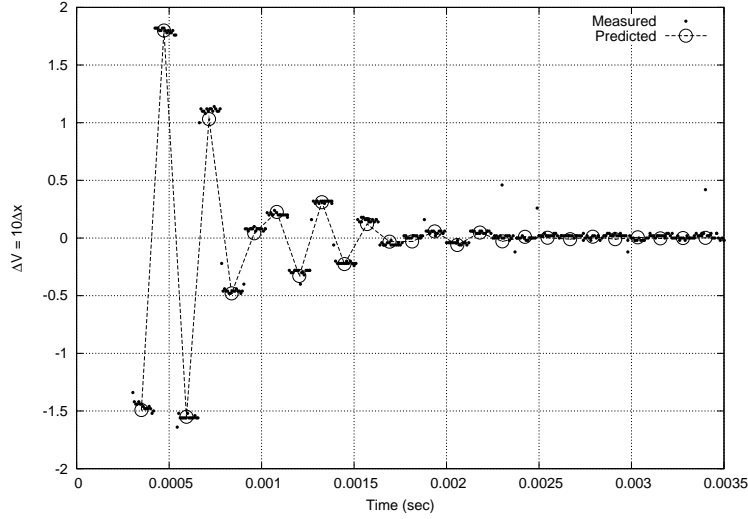


FIG. 6: Data (dots) and prediction (open circles) showing the difference of successive system values $\Delta V_i = 10y_i = 10(x_i - x_{i-1})$ for nonsmooth-convergence, $K = -2.3$. Connecting dashed lines are for visual aid only.

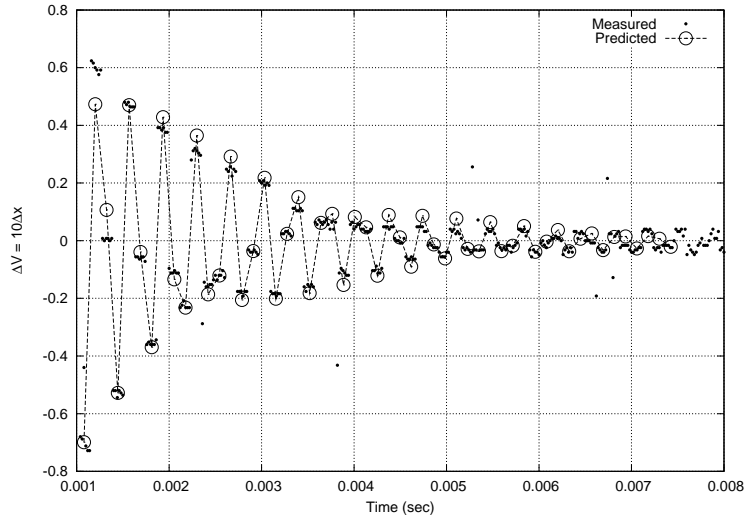


FIG. 7: Data (dots) and prediction (open circles) showing the difference of successive system values $\Delta V_i = 10y_i = 10(x_i - x_{i-1})$ for nonsmooth-convergence, $K = -3.5$. Connecting dashed lines are for visual aid only.